EXTENDED APPLICATIONS OF THE VORTEX LATTICE METHOD

Luis R. Miranda
Lockheed-California Company

SUMMARY

The application of the vortex lattice method to problems not usually dealt with by this technique is considered. It is shown that if the discrete vortex lattice is considered as an approximation to surface-distributed vorticity, then the concept of the generalized principal part of an integral yields a residual term to the vortex-induced velocity that renders the vortex lattice method valid for supersonic flow. Special schemes for simulating non-zero thickness lifting surfaces and fusiform bodies with vortex lattice elements are presented. Thickness effects of wing-like components are simulated by a double vortex lattice layer, and fusiform bodies are represented by a vortex grid arranged on a series of concentrical cylindrical surfaces. Numerical considerations peculiar to the application of these techniques are briefly discussed.

INTRODUCTION

The several versions or variations of the vortex lattice method that are presently available have proven to be very practical and versatile theoretical tools for the aerodynamic analysis and design of planar and non-planar configurations. The success of the method is due in great part to the relative simplicity of the numerical techniques involved, and to the high accuracy, within the limitations of the basic theory, of the results obtained. But most of the work on vortex lattice methods appears to have concentrated on subsonic flow application. The applicability of the basic techniques of vortex lattice theory to supersonic flow has been largely ignored. It is one of the objectives of this paper to show how the vortex lattice method can be easily extended to deal with problems at supersonic Mach numbers with the same degree of success that it enjoys in subsonic flow.

The other objective of this paper is to discuss a couple of schemes by which it is possible to simulate thickness and volume effects by using vortex lattice elements only. This represents an alternative, with somewhat reduced computational requirements, to the method of quadrilateral vortex rings (refs. 1 and 2). The simulation of thickness and volume effects makes possible the computation of the surface pressure distribution on wing-body configurations. The fact that this can be done without having to resort to additional types of singularities, such as sources, results in a simpler digital computer code.

THE BASIC EQUATIONS

Ward has shown, (ref. 3), that the small-perturbation, linearized flow of an inviscid compressible fluid is governed by the three first order vector equations:

$$\nabla \times \overline{v} = \overline{\omega}, \qquad \nabla . \overline{w} = Q, \qquad \overline{w} = \Psi . \overline{v} \tag{1}$$

on the assumption that the vorticity $\overline{\omega}$ and the source intensity Q are known functions of the point whose position vector is $\overline{R}$. The vector $\overline{v}$ is the perturbation velocity with orthogonal cartesian components u, v, and w, and Ψ is a constant symmetrical tensor that for orthogonal cartesian coordinates with the x-axis aligned with the freestream direction has the form

$$\Psi = \begin{bmatrix} 1 - M_\infty^2 & 0 & 0 \\ 0 & 1 & 0 \\ 0 & 0 & 1 \end{bmatrix} \tag{2}$$

where M_∞ is the freestream Mach number. If $\beta^2 = 1-M_\infty^2$, then the vector $\overline{w}$ has the components $\overline{w} = \beta^2 u \overline{i} + v \overline{j} + w \overline{k}$. This vector was first introduced by Robinson (ref. 4), who called it the "reduced current velocity". If $\overline{u}$ denotes the total velocity vector, i.e., $\overline{u} = (u_\infty + u) \overline{i} + v \overline{j} + w \overline{k}$, and ρ the fluid density, then it can be shown that for irrotational and homentropic flow

$$\rho \overline{u} = \rho_\infty \overline{u}_\infty + \rho_\infty \overline{w} + \text{higher order terms} \tag{3}$$

where the subscript ∞ indicates the value of the quantity at upstream infinity, e.g., $\overline{u}_\infty = u_\infty \overline{i}$. Therefore, to a linear approximation, the vector $\overline{w}$ is directly related to the perturbation mass flux as follows:

$$\overline{w} = (\rho \overline{u} - \rho_\infty \overline{u}_\infty) / \rho_\infty \tag{4}$$

The second equation of (1), i.e., the continuity condition, shows that for source-free flows ($Q = 0$), w is a conserved quantity.

Ward has integrated the three first order vector equations directly without having to resort to an auxiliary potential function. He obtained two different solutions for $\overline{v}(\overline{R})$, depending on whether β^2 is positive (subsonic flow), or negative (supersonic flow). These two solutions can be combined formally into a single expression if the following convention is used:

$$K = 2 \quad \text{for} \quad \beta^2 > 0$$

$$K = 1 \quad \text{for} \quad \beta^2 < 0$$

$$R_\beta = \text{Real part of} \left\{ (x-x_1)^2 + \beta^2 \left[(y-y_1)^2 + (z-z_1)^2 \right] \right\}^{1/2}$$

$\int$ = Finite part of integral as defined by Hadamard (refs. 5 and 6).

The resulting solution for the perturbation velocity $\bar{v}$ at the point whose position vector is $\bar{R}_1 = x_1 \bar{i} + y_1 \bar{j} + z_1 \bar{k}$, is given by

$$\bar{v}(\bar{R}_1) = -\frac{1}{2\pi K} \int_S \bar{n} \cdot \bar{w}(\bar{R}) \nabla \frac{1}{R_\beta} \, dS$$

$$+ \frac{\beta^2}{2\pi K} \int_S \{\bar{n} \times \bar{v}(\bar{R})\} \times \frac{\bar{R} - \bar{R}_1}{R_\beta^3} \, dS$$

$$+ \frac{1}{2\pi K} \int_V Q(\bar{R}) \nabla \frac{1}{R_\beta} \, dV + \frac{\beta^2}{2\pi K} \int_V \frac{\bar{R}-\bar{R}_1}{R_\beta^3} \times \bar{\omega}(\bar{R}) \, dV \quad (5)$$

This formula determines the value of $\bar{v}$ within the region V bounded by the surface S. The vector $\bar{n}$ is the unit outward (from the region V) normal to the surface S. Furthermore, it is understood that for supersonic flow only those parts of V and S lying within the domain of dependence (Mach forecone) of the point $\bar{R}_1$ are to be included in the integration.

For source-free ($Q \equiv 0$), irrotational ($\bar{\omega} \equiv 0$) flow, equation (5) reduces to

$$\bar{v}(\bar{R}_1) = -\frac{1}{2\pi K} \int_S \bar{n} \cdot \bar{w}(\bar{R}) \nabla \frac{1}{R_\beta} \, dS + \frac{\beta^2}{2\pi K} \int_S \{\bar{n} \times \bar{w}(\bar{R})\} \frac{\bar{R}-\bar{R}_1}{R_\beta^3} \, dS \quad (6)$$

This is a relation between $\bar{v}$ inside S and the values of $\bar{n} \cdot \bar{w}$ and $\bar{n} \times \bar{v}$ on S, but these two quantities cannot be specified independently on S.

To determine the source-free, irrotational flow about an arbitrary body B by means of equation (6), assume that the surface S coincides with the wetted surface of the body, with any trailing wake that it may have, and with a sphere of infinite radius enclosing the body and the whole flow field about it, namely, $S = S_B + S_W + S_\infty$.

This surface S divides the space into two regions, V_e external to the body, and V_i internal to it. Applying equation (6) to both V_e and V_i, since the integrals over S_∞ converge to zero, the following expression is obtained:

$$\bar{v}(\bar{R}_1) = \frac{1}{2\pi K} \oint_{S_B + S_W} \bar{N} \cdot \Delta \bar{w}\,(\bar{R})\, \nabla \frac{1}{R_\beta}\, dS - \frac{\beta^2}{2\pi K} \oint_{S_B + S_W} \{\bar{N} \times \Delta \bar{v}(\bar{R})\} \times \frac{\bar{R}-\bar{R}_1}{R^3_\beta}\, dS \quad (7)$$

where $\bar{N} = \bar{n}_i = -\bar{n}_e$ is the unit normal to the body, or wake as the case may be, positive from the interior to the exterior of the body, $\Delta \bar{w} = \bar{w}_e - \bar{w}_i$, and $\Delta \bar{v} = \bar{v}_e - \bar{v}_i$. Here the subscripts designate the values of the quantities on the corresponding face of S. The first surface integral can be considered as representing the contribution of a source distribution of surface density $\bar{N} \cdot \Delta \bar{w}$, while the second surface integral gives the contribution of a vorticity distribution of surface density $\bar{N} \times \Delta \bar{v}$.

If the boundary condition of zero mass flux through the surface $S_B + S_W$ is applied to both external and internal flows

$$\bar{N} \cdot \rho \bar{u}_e = \bar{N} \cdot (\rho_\infty \bar{u}_\infty + \rho_\infty \bar{w}_e) = 0$$

$$\bar{N} \cdot \rho \bar{u}_i = \bar{N} \cdot (\rho_\infty \bar{u}_\infty + \rho_\infty \bar{w}_i) = 0 \quad (8)$$

then the condition $\bar{N} \cdot \Delta \bar{w} = 0$ exists over $S_B + S_W$, and the flow field is uniquely determined by

$$\bar{v}(\bar{R}_1) = -\frac{\beta^2}{2\pi K} \oint_{S_B + S_W} \bar{\gamma}\,(\bar{R}) \times \frac{\bar{R}-\bar{R}_1}{R^3_\beta}\, dS \quad (9)$$

where $\bar{\gamma}\,(\bar{R}) = \bar{N} \times \Delta \bar{v}$ is the surface vorticity density.

EXTENSION TO SUPERSONIC FLOW

In order to extend the application of the vortex lattice method to supersonic flow, it is essential to consider the fundamental element of the method, the vortex filament, as a numerical approximation scheme to the integral expression (9) instead of a real physical entity. The velocity field generated by a vortex filament can be obtained by a straightforward limiting process, the result being

$$\bar{v}(\bar{R}_1) = \frac{-\beta^2}{2\pi K} \oint_C \bar{\Gamma} \times \frac{\bar{R}-\bar{R}_1}{R^3_\beta}\, d\ell \quad (10)$$

where $\bar{\Gamma} = \lim_{\substack{\bar{\gamma} \to \infty \\ \delta \to 0}} \bar{\gamma} \cdot \delta$

δ is a dimension normal to γ, and $d\ell$ is the distance element along γ. In the classical vortex lattice method, applicable only to subsonic flow, the vorticity distribution over the body and the wake, i.e., over the surface $S_B + S_W$, is replaced by a suitable arrangement of vortex filaments whose velocity fields are everywhere determined by equation (10). This procedure is no longer appropriate for supersonic flow. For this latter case, it is necessary to go back to equation (9) and to derive an approximation to it. This is done in the following.

If the surface $S_B + S_W$, which defines the body and its wake, is considered as being composed of a large number of discrete flat area elements τ over which the surface vorticity density $\bar{\gamma}$ can be assumed approximately constant, then equation (9) can be approximated by the following equation:

$$\bar{v}(\bar{R}_1) = -\frac{\beta^2}{2\pi K} \sum_{J=1}^{N} \oint_{\tau_J} \bar{\gamma}_J \times \frac{\bar{R}-\bar{R}_1}{R^3_\beta} \, dS \qquad (11)$$

where N is the total number of discrete area elements τ. When the point whose position vector is $\bar{R}_1$ is not part of τ_J, the integral over this discrete area can be approximated by the mean value theorem as follows:

$$\oint_{\tau_J} \bar{\gamma}_J \times \frac{\bar{R}-\bar{R}_1}{R^3_\beta} \, dS = \bar{\gamma}_J \, \delta_J \times \oint_{C_J} \frac{\bar{R}-\bar{R}_1}{R^3_\beta} \, d\ell \qquad (12)$$

where C_J is a line in τ_J parallel to the average direction of $\bar{\gamma}$ in τ_J, δ_J is a distance normal to C_J, and $d\ell$ is the arc length element along C_J. This means that the velocity field induced by a discrete vorticity patch τ_J can be approximated for points outside of τ_J by some mean discrete vortex line whose strength per unit length is $\gamma_J \delta_J$. But if the point $\bar{R}_1$ is part of the discrete area τ, the integral in equation (11) has an inherent singularity of the Cauchy type due to the fact that $\bar{R} = \bar{R}_1$ at some point within τ. In order to evaluate the integral expression for this case, consider a point close to $\bar{R}_1$ but located just above τ by a distance ϵ. As indicated in figure 1, the area of integration in τ is divided into two regions, $A_{\tau-\epsilon}$ and A_ϵ. Obviously, the integral over $A_{\tau-\epsilon}$ has no Cauchy-type singularity, Hadamard's finite part concept being sufficient to perform the indicated integration. Thus,

$$\oint_{\tau} \bar{\gamma} \times \frac{\bar{R}-\bar{R}_1}{R^3_{\beta}}\, dS = \lim_{\epsilon \to 0} \oint_{A_\epsilon} + \lim_{\epsilon \to 0} \oint_{A_{\tau-\epsilon}}$$

$$= \lim_{\epsilon \to 0} I(\epsilon) + \bar{\gamma} A \times \oint_{C} \frac{\bar{R}-\bar{R}_1}{R^3_{\beta}}\, d\ell \qquad (13)$$

The last integral in equation (13) represents the conventional discrete vortex line contribution whose evaluation presents no difficulty. In order to determine the integration denoted by $I(\epsilon)$ assume that, for simplicity, the coordinate system is centered at the point $\bar{R}_1$, and that the x-y plane is determined by the discrete area τ. Then, if γ denotes the modulus of $\bar{\gamma}$,

$$I(\epsilon) = \gamma \oint_{A_\epsilon} \frac{y \sin\Lambda - x \cos\Lambda}{\{x^2 - B^2 (y^2 + \epsilon^2)\}^{3/2}}\, dx\, dy \qquad (14)$$

where Λ is the angle between the y-axis and the direction of the vorticity in τ, and $B^2 = -\beta^2 > 0$ (supersonic flow). The components of the vector cross product $\bar{\gamma} \times (\bar{R}-\bar{R}_1) = \bar{\gamma} \times \bar{R}$ which are not normal to the plane of τ have been left out of equation (14) because, when the limit operation $\epsilon \to 0$ is carried out, they will vanish. The area A_ϵ is bounded by a line parallel to the vorticity direction going through $x = -(1+B)\epsilon$ and by the intersection of the Mach forecone from the point (o, o, ϵ) with the τ-plane, consequently, if the integration with respect to x is performed first,

$$I(\epsilon) = \gamma \cos\Lambda \oint_{\lambda_1}^{\lambda_2} \left\{ \oint_{ty-(1+B)\epsilon}^{-B\sqrt{y^2+\epsilon^2}} \frac{ty - x}{\{x^2 - B^2 (y^2 + \epsilon^2)\}^{3/2}}\, dx \right\} dy \qquad (15)$$

where $t = \tan\Lambda$, and λ_1, λ_2 are the values of y corresponding to the intersection of the line $x = ty - (1+B)\epsilon$ with the hyperbola $x = -B\sqrt{y^2 + \epsilon^2}$. Let $\phi = \epsilon^2(1+2B) - 2(1+B)\epsilon ty - (B^2 - t^2) y^2$, then the finite part of the x-integration yields

$$I(\epsilon) = \gamma \cos\Lambda \oint_{\lambda_1}^{\lambda_2} \left\{ \frac{ty\,(ty-(1+B)\epsilon)}{B^2 (y^2 + \epsilon^2)\sqrt{\phi}} - \frac{1}{\sqrt{\phi}} \right\} dy$$

$$= \frac{\gamma \cos\Lambda}{B^2} \int_{\lambda_1}^{\lambda_2} \left\{ \frac{B^2\epsilon-(1+B)\ \epsilon t y-(B^2-t^2)y^2}{y^2+\epsilon^2} \right\} \frac{dy}{\sqrt{\phi}} \qquad (16)$$

Since ϵ is a very small quantity, the variation of y in the interval (λ_1, λ_2) is going to be equally small, and, therefore, the quantity within brackets in the last integrand of equation (16) can be replaced by a mean value and taken outside of the integral sign. The same is not true of the term $1/\sqrt{\phi}$ since it will vary from ∞ for $y = \lambda_1$, go through finite values in the integration interval, and then again increase to ∞ for $y = \lambda_2$. With this in mind, and if $\tilde{y}$ denotes a mean value of y, $I(\epsilon)$ can be written as

$$I(\epsilon) = \frac{\gamma \cos\Lambda}{B^2} \frac{B^2\epsilon-(1+B)\ \epsilon t\tilde{y} - (B^2-t^2)\ \tilde{y}^2}{\tilde{y}^2+\epsilon^2} \int_{\lambda_1}^{\lambda_2} \frac{dy}{\sqrt{\phi}} \qquad (17)$$

But λ_1, λ_2 are the roots of $ty-\epsilon = -B\sqrt{y^2+\epsilon^2}$, i.e., they are the roots of the polynomial denoted by ϕ. Thus

$$\sqrt{\phi} = \sqrt{\epsilon^2(1+2B)-2(1+B)\epsilon t y\ -(B^2-t^2)\ y^2} = \sqrt{B^2-t^2}\ .\ \sqrt{(\lambda_1-y)(y-\lambda_2)} \qquad (18)$$

Introducing this expression for $\sqrt{\phi}$ into (17), and taking the limit $\epsilon \to o$, the following value for $I(\epsilon)$ is obtained:

$$I(o) = \lim_{\epsilon \to o} I(\epsilon) = -\frac{\gamma \cos\Lambda}{B^2} \sqrt{B^2-t^2} \int_{\lambda_1}^{\lambda_2} \frac{dy}{\sqrt{(\lambda_1-y)(y-\lambda_2)}} \qquad (19)$$

The integral appearing in equation (19) can be easily evaluated by complex variable methods; its value is found to be

$$\int_{\lambda_1}^{\lambda_2} \frac{dy}{\sqrt{(\lambda_1-y)(y-\lambda_2)}} = \pi \qquad (20)$$

The contribution of the inherent singularity to the velocity field induced by vorticity patch $\mathcal{T}$, within $\mathcal{T}$, denoted herein by w^*, is therefore given by

$$w^* = -\frac{\beta^2}{2\pi} \lim_{\epsilon \to o} I(\epsilon) = -\frac{\gamma \cos \Lambda}{2} \sqrt{B^2 - t^2} \qquad (21)$$

This contribution is perpendicular to the plane of $\mathcal{T}$, and it has only physical meaning when $B^2 > t^2$, i.e., when the vortex lines are swept in front of the Mach lines. It is expression (21), taken in conjunction with equation (12), that makes the vortex lattice method applicable to supersonic flow.

MODELING OF LIFTING SURFACES WITH THICKNESS

The method of quadrilateral vortex rings placed on the actual body surface (ref. 1) provides a way of computing the surface pressure distribution of arbitrary bodies using discrete vortex lines only. Numerical difficulties may occur when the above method is applied to the analysis of airfoils with sharp trailing edges due to the close proximity of two vortex surfaces of nearly parallel direction. An alternative approach, requiring somewhat less computer storage and easier to handle numerically, consists in using a double, or biplanar, sheet of swept horseshoe vortices to model a lifting surface with thickness, as shown schematically in figure 2. This constitutes an approximation to the true location of the singularities, similar in nature to the classical lifting surface theory approximation of a cambered sheet.

All the swept horseshoe vortices, and their boundary condition control points, corresponding to a given surface, upper or lower, are located in a same plane. The upper and lower surface lattice planes are separated by a gap which represents the chordwise average of the airfoil thickness distribution. The results are not too sensitive to the magnitude of this gap; any value between one half to the full maximum chordwise thickness of the airfoil has been found to be adequate, the preferred value being two thirds of the maximum thickness. Furthermore, the gap can vary in the direction normal to the x-axis to allow for spanwise thickness taper. On the other hand, the chordwise distribution, or spacing, of the transverse elements of the horseshoe vortices have a significant influence on the accuracy of the computed surface pressure distribution. For greater accuracy, for a given chordwise number of horseshoe vortices, the transverse legs have to be longitudinally spaced according to the 'cosine' distribution law

$$x_J^v - x_o = \frac{c}{2}\left[1 - \cos\left(\pi \frac{2J-1}{2N}\right)\right] \qquad (22)$$

where $x_J^v - x_o$ represents the distance from the leading edge to the midpoint of the swept leg of the Jth horseshoe vortex, c is the length of the local chord running through the midpoints of a given chordwise strip, and N is the number of horseshoe vortices per strip. The chordwise control point location

corresponding to this distribution of vortex elements is given by

$$x_J^C - x_o = \frac{c}{2}\left[1 - \cos\left(\pi \frac{J}{N}\right)\right] \tag{23}$$

The control points are located along the centerline, or midpoint line, of the chordwise strip (fig. 3). Lan has shown (ref. 7) that the chordwise 'cosine' collocation of the lattice elements, defined by equations (22) and (23), greatly improve the accuracy of the computation of the effects due to lift. His results are directly extendable to the computation of surface pressure distributions of wings with thickness by the 'biplanar' lattice scheme presented herein.

The small perturbation boundary condition

$$\bar{v} \cdot \bar{n}' = -\bar{u}_\infty \cdot \bar{n} \tag{24}$$

is applied at the control points. In equation (24), $\bar{n} = \ell\bar{i} + m\bar{j} + n\bar{k}$, and $\bar{n}' = m\bar{j} + n\bar{k}$, where ℓ, m, and n are the direction cosines of the normal to the actual airfoil surface. Equation (24) implies that $|\ell u| \ll |mv + nw|$. The use of the small perturbation boundary condition is consistent with the present 'biplanar' approach to the simulation of thick wings.

MODELING OF FUSIFORM BODIES

The modeling of fusiform bodies with horseshoe vortices requires a special concentrical vortex lattice if the simulation of the volume displacement effects, and the computation of the surface pressure distribution, are to be carried out. To define this lattice, it is necessary to consider first an auxiliary body, identical in cross-sectional shape and longitudinal area distribution to the actual body, with a straight barycentric line, i.e., without camber. The cross-sectional shape of this auxiliary body is then approximated by a polygon whose sides determine the transverse legs of the horseshoe vortices. The vertices of the polygon and the axis of the auxiliary body (which by definition is rectilinear (zero camber) and internal to all possible cross sections of the body) define a set of radial planes in which the bound trailing legs of the horseshoe vortices lie parallel to the axis (fig. 4). As the body cross section changes shape along its length, the corresponding polygon is allowed to change accordingly, but with the constraint that the polygonal vertices must always lie in the same set of radial planes. The axial spacing of the cross-sectional planes that determine the transverse vortex elements, or polygonal rings, follows the 'cosine' law of equation (22). The boundary condition control points are located on the auxiliary body surface, and in the bisector radial planes, with their longitudinal spacing given by equation (23).

The boundary condition to be satisfied at these control points is the zero mass flux equation

$$\bar{w} \cdot \bar{n} = - \bar{u}_\infty \cdot \bar{n} \qquad (25)$$

where all the components of the scalar product $\bar{w} \cdot \bar{n} = \beta^2 \ell u + mv + nw$ are to be retained. Thus, equation (25) is a higher order condition than equation (24). The use of this higher order boundary condition, within the framework of a linearized theory, is not mathematically consistent. Therefore, it can only be justified by its results rather than by a strict mathematical derivation. In the present treatment of fusiform bodies, it has been found that the use of higher order, or 'exact' boundary conditions is a requisite for the accurate determination of the surface pressure distribution.

The fact that the vector $\bar{w}$, instead of $\bar{v}$, appears in the left hand member of equation (25) requires some elaboration. First, it should be pointed out that for small perturbations $\bar{w} \cdot \bar{n} \cong \bar{v} \cdot \bar{n}'$. Furthermore, for incompressible flow ($\beta = 1$), the vector $\bar{w}$ is identical to the perturbation velocity $\bar{v}$. Consequently, the boundary condition equation (24) is consistent with the continuity equation, $\nabla \cdot \bar{w} = 0$, to a first order for compressible flow, and to any higher order for incompressible flow. But when a higher order boundary condition is applied in compressible flow to a linearized solution, it should be remembered that this solution satisfies the conservation of $\bar{w}$, not of $\bar{v}$, i.e., $\nabla \cdot \bar{w} = 0$. Thus, the higher order boundary condition should involve the reduced current velocity, or perturbation mass flux, vector $\bar{w}$, as in equation (25), rather than the perturbation velocity vector $\bar{v}$.

The body camber, which was eliminated in the definition of the auxiliary body, is taken into account in the computation of the direction cosines ℓ, m, and n, which are implicit in equation (25). Therefore, the effect of camber is represented in the boundary condition but ignored in the spatial placement of the horseshoe elements. This scheme will give a fair approximation to cambered fusiform bodies provided that the amount of body camber is not too large.

THE GENERALIZED VORTEX LATTICE METHOD

Description of Method

The three features discussed above, i.e., the inclusion of the vorticity-induced residual term w^* for supersonic flow, the 'biplanar' scheme for representing thickness, and the use of a vortex grid of concentrical polygonal cylinders for the simulation of fusiform bodies, have been implemented in a computational procedure herein known as the Generalized Vortex Lattice (GVL) method. The GVL method has been codified in a Fortran IV computer program (VORLAX), which has been widely utilized throughout the Lockheed-California Company as an efficient aerodynamic design tool for advanced aircraft configurations in subsonic and supersonic flows.

The basic element of the method is the swept horseshoe vortex with 'bound' and 'free' legs. In the present version of the method, the free legs may trail to downstream infinity in any arbitrary, but predetermined, direction. The lattice formed by the bound legs of the horseshoe vortices is laid out on the proper cylindrical surfaces, the trailing legs being parallel to the x-axis. Figure 5 illustrates schematically the representation of a simple wing-body configuration within the context of the present method. The streamwise arrangement of the lattice follows the 'cosine' distribution law (eq. (22)), whereas the spanwise, or cross-flow, spacing of the trailing legs can be arbitrarily specified. To each horseshoe vortex there corresponds an associated control point, placed midway between the bound trailing legs of the horseshoe and longitudinally spaced according to equation (23).

The velocity field induced by the elementary horseshoe vortex is derived from equation (12), and it includes the contribution given by equation (21) when the velocity induced by a horseshoe at its own control point is evaluated at supersonic Mach numbers. This velocity field is used to generate the coefficients of a system of linear equations relating the unknown vortex strengths to the appropriate boundary condition at the control points. This linear system is solved by either a Gauss-Seidel iterative procedure (ref. 8), or by a vector orthogonalization technique (ref. 9).

The pressure coefficients are computed in terms of the perturbation velocity components. Force and moment coefficients are determined through a numerical integration process. Due account is taken of the leading edge suction through the application of Lan's procedure (ref. 7), which the GVL method directly extends to supersonic flow.

Numerical Considerations

At supersonic Mach humbers, the velocity induced by a discrete horseshoe vortex becomes very large in the very close proximity of the envelope of Mach cones generated by the transverse leg of the horseshoe. At the characteristic envelope surface itself, the induced velocity correctly vanishes, due to the finite part concept. This singular behavior of the velocity field occurs only for field points off the plane of the horseshoe. For the planar case, the velocity field is well behaved in the vicinity of the characteristic surface. A simple procedure to treat this numerical singularity consists of defining the characteristic surfaces by the equation

$$(x-x_1)^2 = C\,B^2\left\{(y-y_1)^2 + (z-z_1)^2\right\} \qquad (26)$$

where C is a numerical constant whose value is greater than, but close to, 1. It has been found that this procedure yields satisfactory results, and that these results are quite insensitive to reasonable variations of the parameter C.

Another numerical problem, peculiar to the supersonic horseshoe vortex, exists in the planar case (field point in the plane of the horseshoe) when the field point is close to a transverse vortex leg swept exactly parallel to the Mach lines (sonic vortex), while the vortex lines immediately in front of and behind this sonic vortex are subsonic and supersonic, respectively. This problem can be handled by replacing the boundary condition equation for such sonic vortex with the averaging equation

$$-\gamma_{I^*-1} + 2\,\gamma_{I^*} - \gamma_{I^*+1} = 0 \qquad (27)$$

where γ_{I^*} is the circulation strength of the critical horseshoe vortex, and γ_{I^*-1} and γ_{I^*+1} are the respective circulation values for the fore-and-aft adjacent subsonic and supersonic vortices.

The axialwash induced velocity component (u) is needed for the computation of the surface pressure distribution, and for the formulation of the boundary condition for fusiform bodies. When the field point is not too close to the generating vorticity element, the axialwash is adequately described by the conventional discrete horseshoe vortex representation. But if this point is in the close vicinity of the generating element, as may occur in the biplanar and in the concentrical cylindrical lattices of the present method, the error in the computation of the axialwash due to the discretization of the vorticity becomes unacceptable. This problem is solved by resorting to a vortex-splitting technique, similar to the one presented in reference 10. Briefly, this technique consists of computing the axialwash induced by the transverse leg of a horseshoe as the summation of several transverse legs longitudinally redistributed, according to an interdigitation scheme, over the region that contains the vorticity represented by the single discrete vortex. This is done only if the point at which the axialwash value is required lies within a given near field region surrounding the original discrete vortex.

COMPARISON WITH OTHER THEORIES AND EXPERIMENTAL RESULTS

Conical flow theory provides a body of 'exact' results, within the context of linearized supersonic flow, for some simple three-dimensional configurations. These exact results can be used as bench mark cases to evaluate the accuracy of numerical techniques. This has been done rather extensively for the GVL method, and very good agreement between it and conical flow theory has been observed in the computed aerodynamic load distribution and all force and moment coefficients. Only some typical comparisons are presented in this paper, figures 6 through 9.

Finally, the capability of computing surface pressure distributions by the method of this paper is illustrated in figures 10 and 11.

CONCLUDING REMARKS

It has been shown that vortex lattice theory can be extended to supersonic flow if due account is taken of the principal part of the surface vorticity integral. Furthermore, special vortex lattice layouts, which allow the simulation of thickness and volume with horseshoe vortices, have been presented. All this greatly enhances the value of vortex lattice theory as a computationally efficient design and analysis tool, as exemplified by its extensive use at the Lockheed-California Company, discussion of which has been precluded by space limitations.

REFERENCES

1. Maskew, B.: Calculation of the Three-Dimensional Potential Flow Around Lifting Non-Planar Wings and Wing-Bodies Using a Surface Distribution of Quadrilateral Vortex-Rings. Loughborough University of Technology TT 7009, 1970.

2. Tulinius, J.; Clever, W.; Niemann, A.; Dunn, K.; and Gaither, B.: Theoretical Prediction of Airplane Stability Derivatives at Subcritical Speeds. North American Rockwell NA-72-803, 1973. (Available as NASA CR-132681.)

3. Ward, G. N.: Linearized Theory of Steady High-Speed Flow. Cambridge University Press, 1955.

4. Robinson, A.: On Source and Vortex Distributions in the Linearized Theory of Steady Supersonic Flow. Quart. J. Mech. Appl. Math. I, 1948.

5. Lomax, H.; Heaslet, M. A.; and Fuller, F. B.: Integrals and Integral Equations in Linearized Wing Theory. NACA Report 1054, 1951.

6. Hadamard, J.: Lectures on Cauchy's Problem in Linear Partial Differential Equations. Yale University Press, 1923.

7. Lan, E. C.: A Quasi-Vortex-Lattice Method in Thin Wing Theory. Journal of Aircraft, Sept. 1974.

8. Bratkovich, A.; and Marshall, F. J.: Iterative Techniques for the Solution of Large Linear Systems in Computational Aerodynamics. Journal of Aircraft, Feb. 1975.

9. Purcell, E. W.: The Vector Method of Solving Simultaneous Linear Equations. Journal of Mathematical Physics, Vol. 23, 1953.

10. Lan, E. C.; and Campbell, J. F.: Theoretical Aerodynamics of Upper-Surface-Blowing Jet-Wing Interaction. NASA TN D-7936, Nov. 1975.

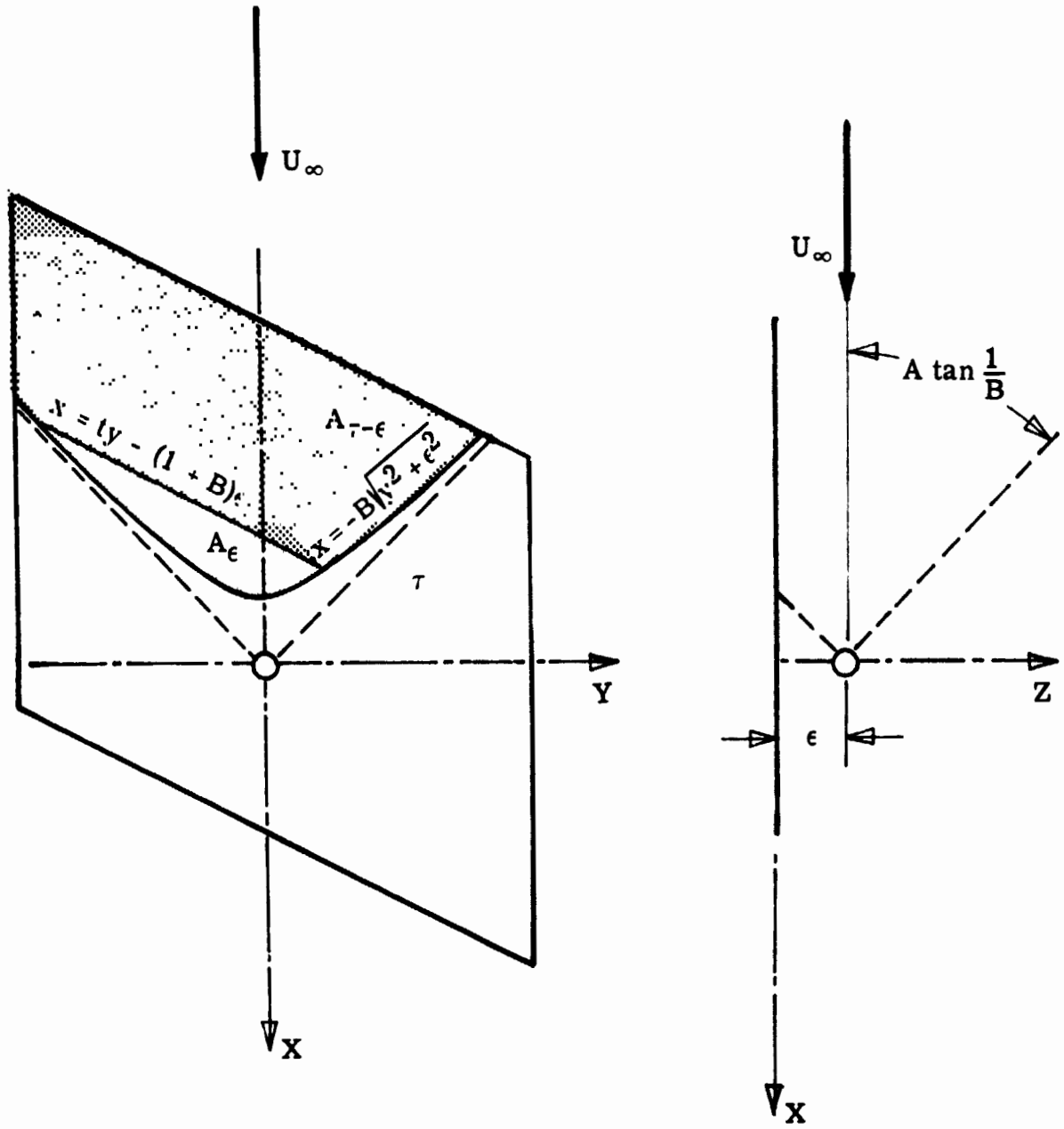

Figure 1.- Definition of integration regions for the computation of principal part.

ACTUAL WING PANEL

BOUNDARY CONDITION: $\bar{w}\cdot\bar{n}' = \bar{v}\cdot\bar{n}' = -\bar{u}_\infty\cdot\bar{n}\ ;\ \bar{n}' = m\bar{j} + n\bar{k}$

THIN PANEL LATTICE

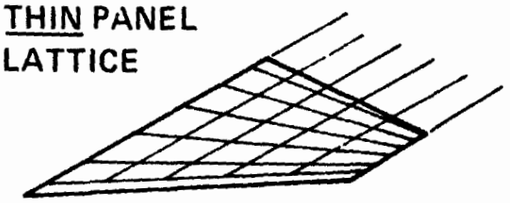

THICK PANEL LATTICE

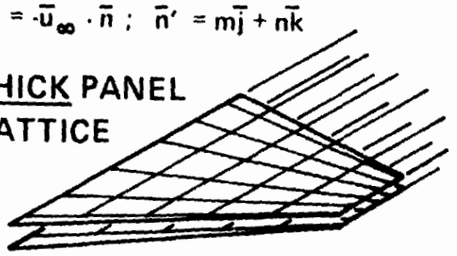

CHORDWISE DISTRIBUTION OF VORTEX LINES: $\dfrac{X_j^v - X_o}{C} = \dfrac{1}{2}\left|1 - \cos\left(\pi\,\dfrac{2J-1}{2N}\right)\right|$

CHORDWISE DISTRIBUTION OF B.C. CONTROL POINTS: $\dfrac{X_j^c - X_o}{C} = \dfrac{1}{2}\left|1 - \cos\left(\pi\,\dfrac{J}{N}\right)\right|$

Figure 2.- Modeling of thick wing with horseshoe vortices.

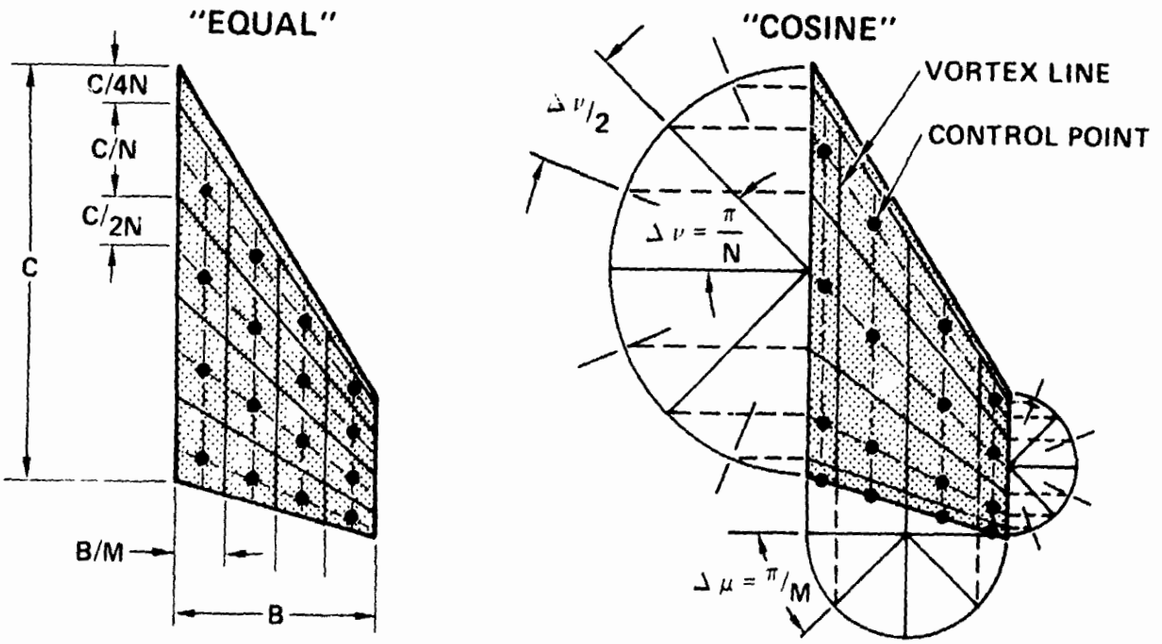

Figure 3.- Vortex lattice collocation.

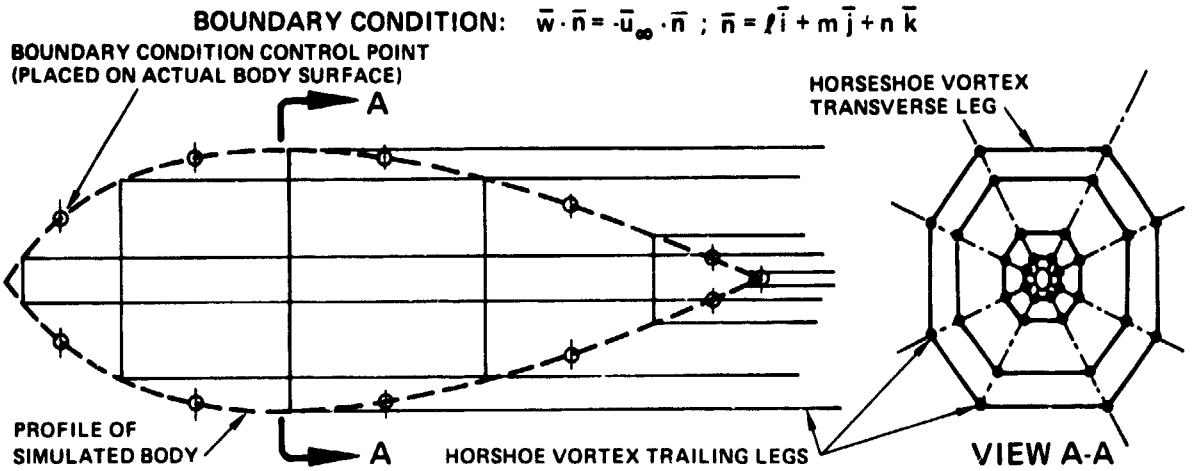

AXIAL DISTRIBUTION OF VORTEX LINES: $\frac{X_j^v - X_o}{L} = \frac{1}{2}\left|1 - \cos\left(\pi\,\frac{2J-1}{2N}\right)\right|$

AXIAL DISTRIBUTION OF B.C. CONTROL POINTS: $\frac{X_j^c - X_o}{L} = \frac{1}{2}\left|1 - \cos\left(\pi\,\frac{J}{N}\right)\right|$

Figure 4.- Modeling of fusiform body with horseshoe vortices.

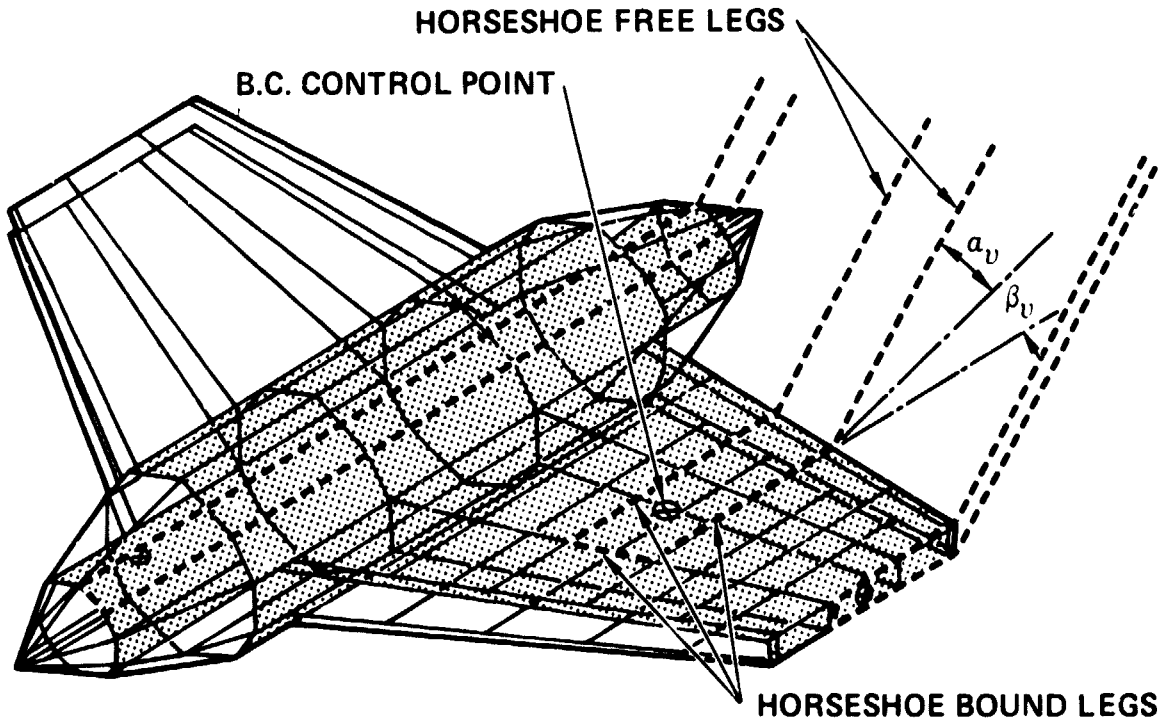

Figure 5.- Generalized vortex lattice model of wing-body configuration.

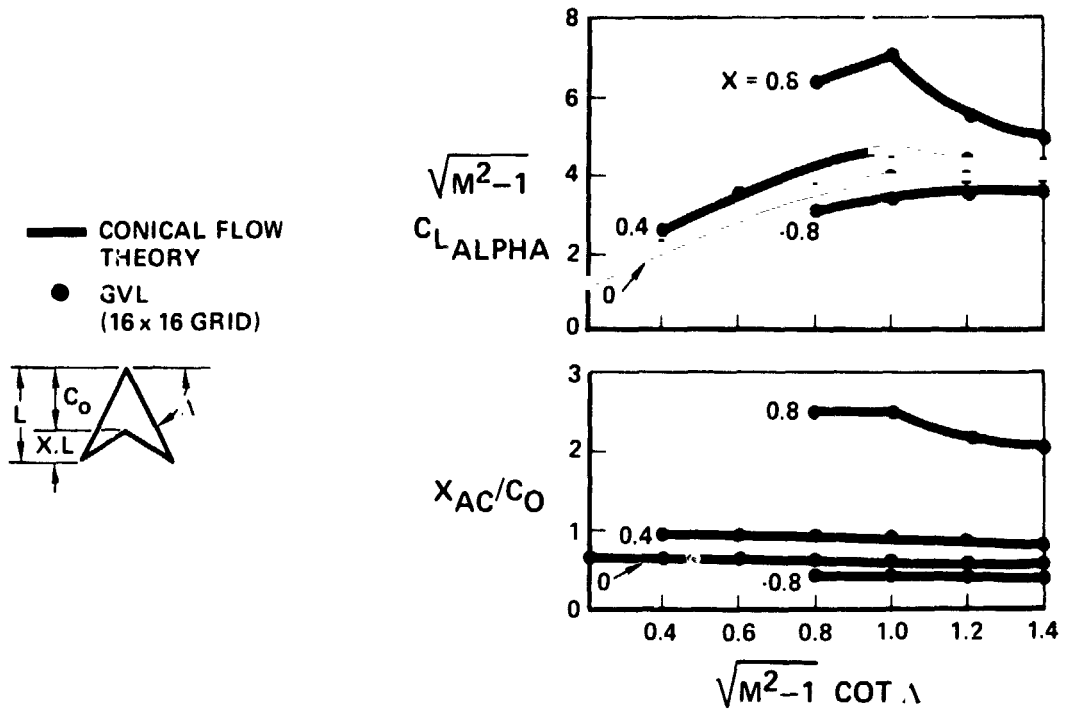

Figure 6.- Theoretical comparison of arrow wing lift slope and aerodynamic center location.

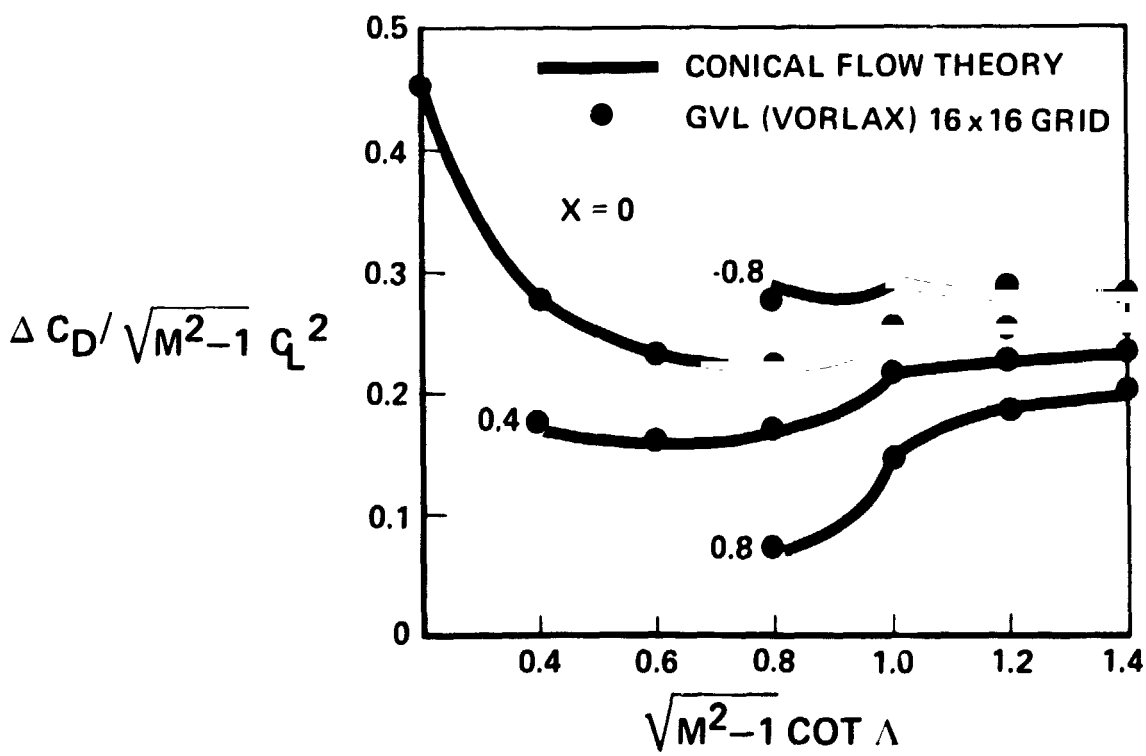

Figure 7.- Theoretical comparison of arrow wing drag-due-to-lift factor.

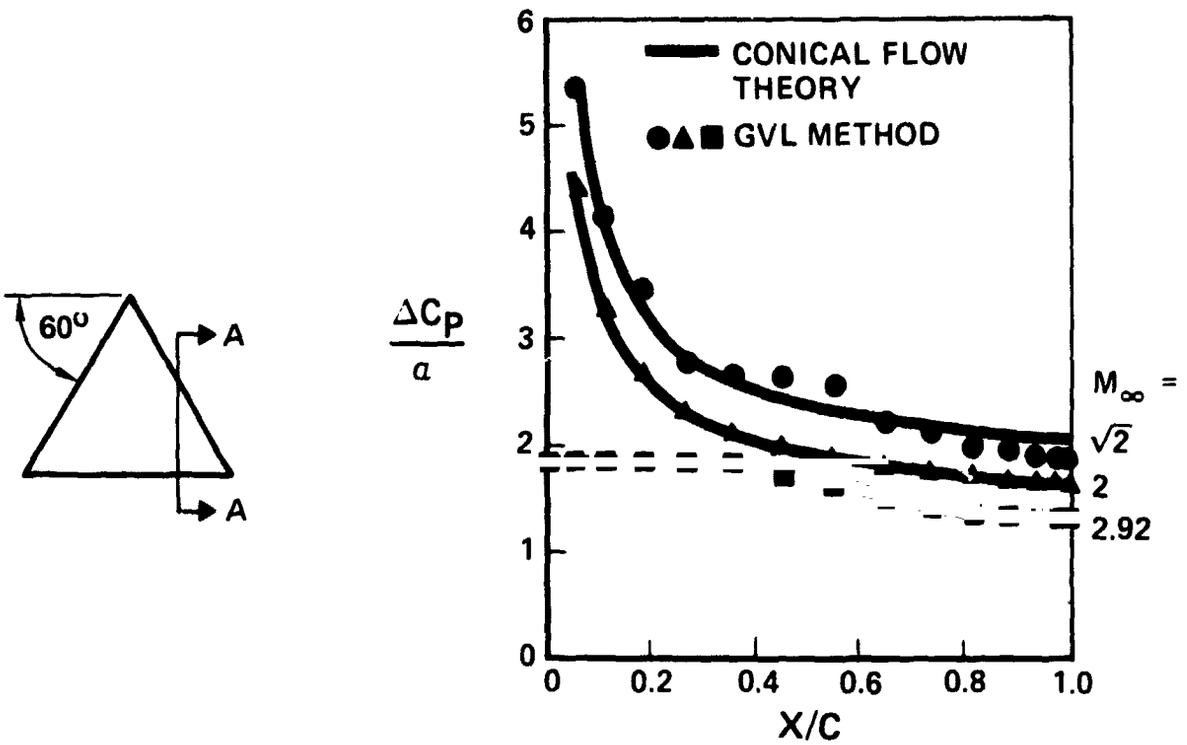

Figure 8.- Theoretical comparison of chordwise loading for delta wing.

SWEEP=59° ; ASPECT RATIO = 1.92 MACH NUMBER= $\sqrt{2}$

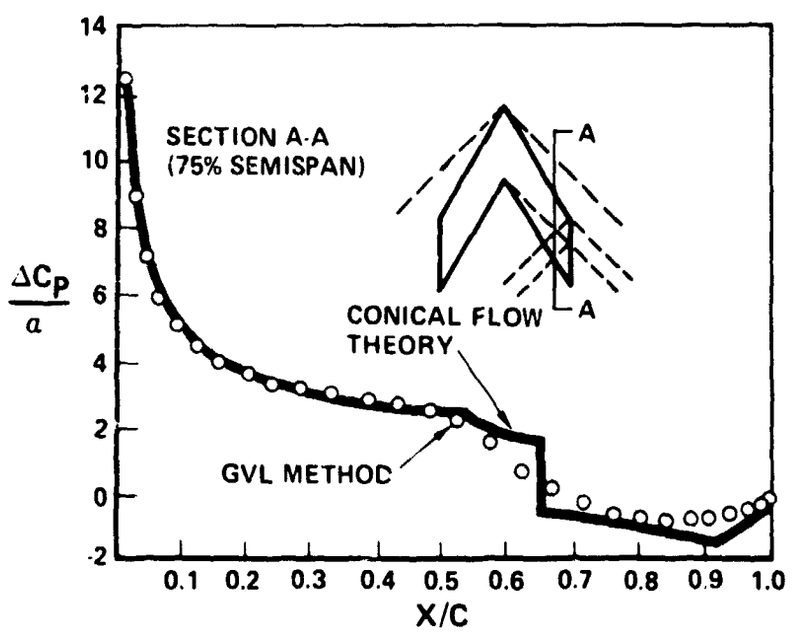

Figure 9.- Theoretical comparison of chordwise loading for sweptback rectangular wing.

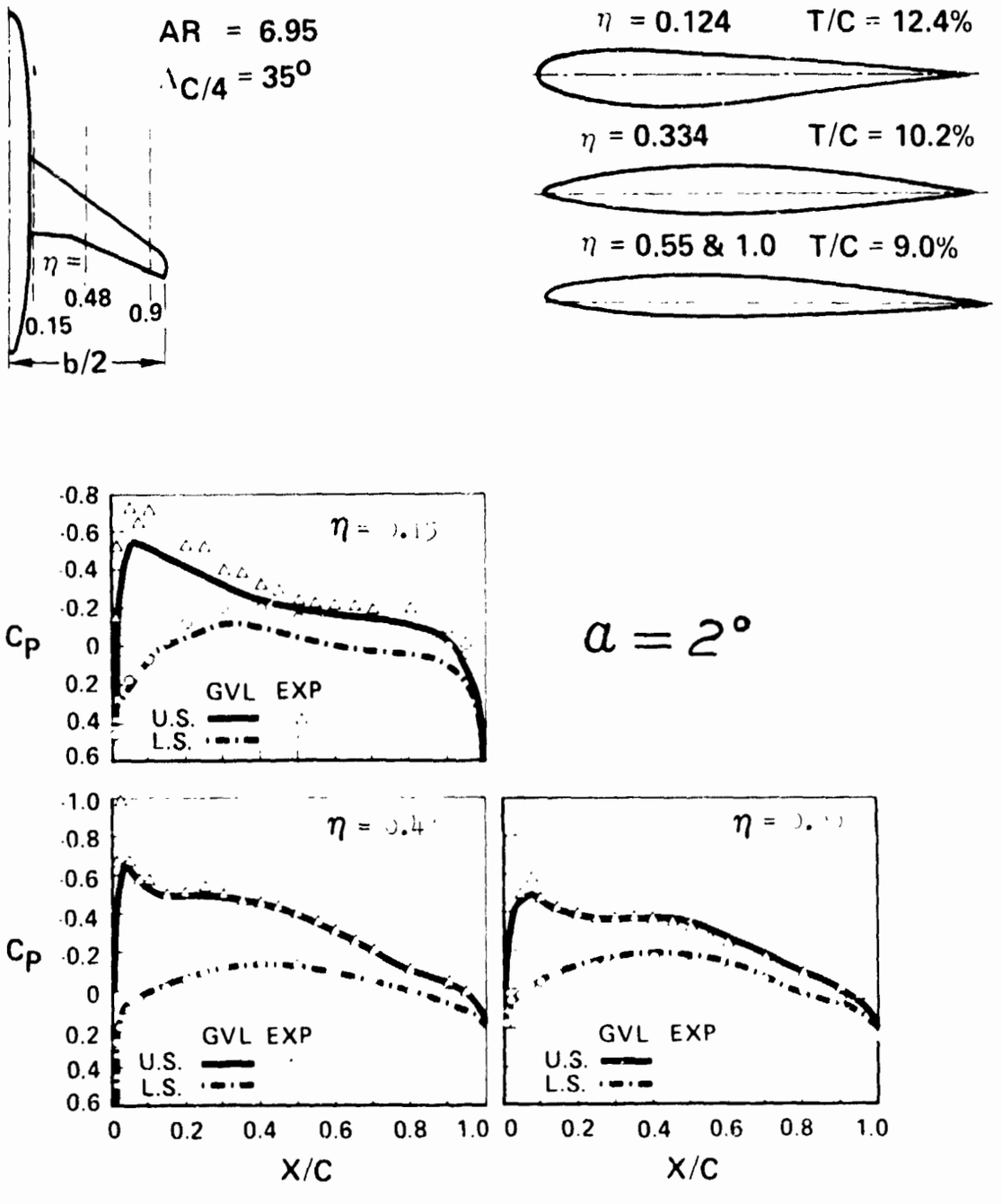

Figure 10.- Comparison with experimental pressure distribution on wing-body model at Mach = 0.5.

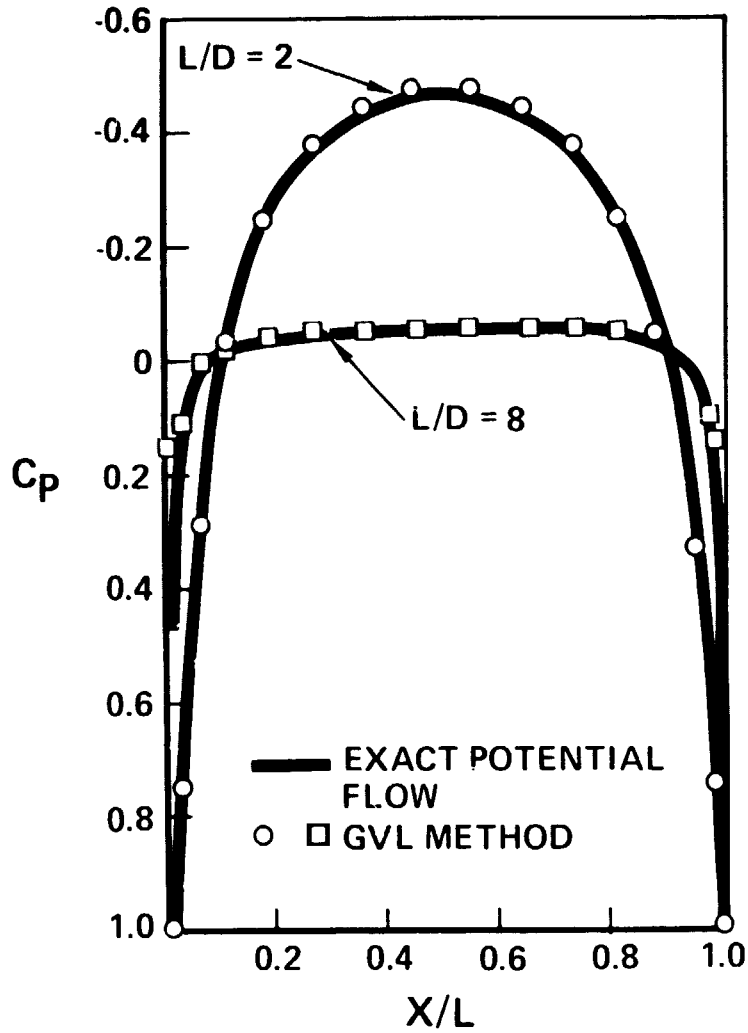

Figure 11.- Theoretical comparison of pressure distribution on ellipsoids at zero angle of attack in incompressible flow.